THE PUBLISHING HOUSE
OF THE ROMANIAN ACADEMY

PROCEEDINGS OF THE ROMANIAN ACADEMY, Series A,
Volume 26, Number x/2025, pp. 000–000

THE SCALE EFFECT OF FFF-PRINTED POLYLACTIC ACID PARTS UNDER QUASI-STATIC COMPRESSION

Cristina VĂLEAN[1], Sergiu-Valentin GALAȚANU[2], Nicușor-Alin SÎRBU[3], Emanoil LINUL[2]

[1] Politehnica University Timisoara, Research Institute for Renewable Energies,
Musicescu Gavril Str., No. 138, 300 774, Timisoara, Romania
[2] Politehnica University Timisoara, Department of Mechanics and Strength of Materials,
1 Mihai Viteazu Avenue, 300222, Timisoara, Romania
[3] National R&D Institute of Welding and Material Testing ISIM Timisoara, 30 Mihai Viteazu Avenue, 300222, Timisoara, Romania
Corresponding author: Emanoil LINUL, E-mail: emanoil.linul@upt.ro

Abstract. The paper presents the scale effect on the compressive behavior of additively manufactured Polylactic Acid (PLA) parts. The experimental setup is based on quasi-static compression tests performed on parts manufactured by Fused Filament Fabrication (FFF). The mechanical tests were carried out on cubic parts (side of 10, 30, 50, 70, 90 and 110 mm) with a test speed of 10 mm/min, at room temperature and under displacement control. The main investigated properties were compressive modulus, compressive strength and energy absorption, presenting at the same time discussions related to the physical properties (print time, dimensional accuracy and mass of the parts). The obtained results show a strong dependence of the properties on the size of the FFF-printed PLA parts. As expected, the physical characteristics increase with the increase in the size of the parts, except for the dimensional accuracy shows low errors and close values. On the other hand, mechanical properties decrease with the increase in the size of the printed parts, compressive strength and energy absorption showing a more pronounced decrease.

Keywords: Fused Filament Fabrication, Polylactic Acid, compression properties, scale effect.

1. INTRODUCTION

Rapid prototyping is an industrial production process that allows the construction of complex geometries and shapes, sometimes impossible to achieve through another processes [1-3]. One of the advantages of rapid prototyping is given by the fact that a wide range of materials can be used to obtain the desired parts [4, 5]. Some examples could be polymers, ceramics, metals and their alloys, as well as biocompatible materials [6-8]. Of course, the industries in which this technology can be used are numerous, from the automotive, construction, sports, to the military, aerospace and medical industries [9-11]. One of the most well-known and used manufacturing processes is Fused Filament Fabrication (FFF), known for its accuracy, speed and competitive cost [12, 13]. Also, it is known for the wide range of materials that can be used in the production of related parts (Polylactic Acid-PLA, Thermoplastic Polyurethane-TPU, Acrylonitrile Butadiene Stirene-ABS, Polyethylene Terephthalate Glycol-PETG, nylon, etc.), the most used of all being PLA [14-16].

Most of the research carried out through the FFF process focuses on the tensile and flexural mechanical behavior. In this sense, optimization studies are carried out regarding the most important process parameters (infill pattern-IP, layer thickness-LT, printing speed-PS, printing orientation-PO, infill density-ID, printing temperature-PT, etc.) [17-19]. Only a small part of the investigations in the specialized literature is attributed to the compression behavior. Oudah et al. [20] investigated the effect of process parameters in the case of compression tests of ABS specimens. They concluded that, among the three investigated parameters (ID, IP and LT), the one that affects the compressive strength to the greatest extent is the ID, its contribution being 82%. The three previously mentioned parameters were also investigated by Ali et al. [21], who follow both the tensile and compressive behavior of the samples obtained by FFF, the best values being obtained for the samples with 60%-ID, Gyroid-IP and 0.05 mm-LT. Another extensive study using different materials (PETG, PLA and ABS), with two different PO angles, was carried out by Erdaș et al. [22]. They observed that the

highest force values, in the case of compression tests, are obtained for PLA, followed by ABS and PETG. Vidakis et al. [23] investigate energy consumption compared to strength in the case of PLA samples subjected to compression. They conclude that the most influential factors in compressive strength are ID and PO. In addition, they determine the best agreement between mechanical resistance and energy efficiency. In addition to the mechanical compression behavior of PLA, Vidakis et al. [24] also investigate that of PLA with graphene, in the FFF process. The study shows approximately the same behavior for both materials. Moreover, the authors also study the dielectric of the materials, obtaining an increase in the parameter values in the case of PLA with graphene. Claudio et al. [25] investigate fatigue behavior (compression-compression), traction and creep (compression). They obtained a linear dependence between the compressive strength and the density of the specimens, but do not find any correlation for fatigue.

As can be seen, most studies focus on standardized tensile, compression and bending samples. However, the extrapolation of laboratory data (on samples) to practical applications (real structures) faces a rather complex process. The present work investigates the scale effect of 3D printed components under compression loads. These results help the designers in estimating the laboratory-reality transition as accurately as possible. The emphasis is placed on strength properties and energy absorption performance. At the same time, data are presented with reference to the elastic and deformation characteristics of the samples.

2. MATERIALS AND METHODS

A PLA filament was used to manufacture the parts under investigation. The PLA filament was chosen due to its good physical and mechanical characteristics (high properties, biodegradable, recyclable, non-toxic) [3]. The filament was purchased in a roll, with a density of 1.24 g/cm^3 and a diameter of 1.75 mm.

The supplier reported values for flexural strength of 108 MPa, tensile strength of 60 MPa and elongation at break of 160%. The filament requires a printing temperature between 190-230 °C, it becomes soft around 60 °C [10].

Figure 1 shows the steps taken from the design of the parts to their testing. To investigate the compression scale effect, cubic parts were adopted (Figure 1a). The parts had a side between 10 and 110 mm, with a step of 20 mm. To simplify the discussion, the cube with a side of 10 mm was denoted by C10, and so on until C110. The SolidWorks® software was used to model the parts.

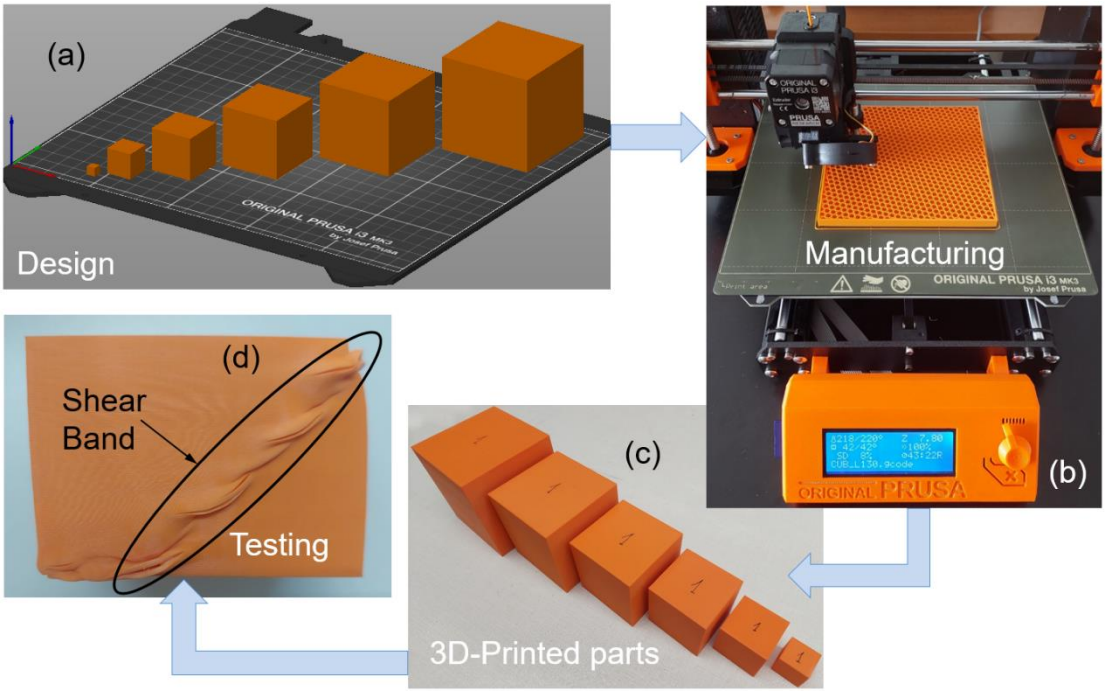

Fig. 1 – Developing cycle for samples from CAD to testing

The manufacturing process was carried out on an Original Prusa i3 MK3 printer (Figure 1b), the parts being processed in its software (Ultimaker Cura 5.0.0). The manufactured parts presented a high dimensional accuracy (Figure 1c), an aspect that will be seen in the discussions presented in Section 3. The main parameters are presented in Table 1. The optimal parameters of the specimens such as ID, IP, LT, PS and PO were obtained by the authors in previous researches [6, 10, 12]. In this study, the ideal values, the optimized ones, were used. For the reproducibility of the results, four samples were tested for each size of the cube.

Table 1 Parameters used in the FFF process of parts:

Parameter	Unit	Value
Infill density	%	30
Infill pattern	-	Star
Print speed	mm/s	20
Bed temperature	°C	42
Extruder temperature	°C	220
Layer thickness	mm	0.2
Number of shells	-	3
Top/bottom solid layers	-	4
Nozzle diameter	mm	0.6

A universal testing machine EDZ 40 no. 990.02/8-78 was used to perform the tests at a speed of 10 mm/min. The machine uses the software of the basic TestXpert II programme to process the results of the compression test. The test machine contains a P340/7.5 ByS hydraulic system. To calibrate hydraulic testing machines, the software TestXpert II standard package is used. The mechanical tests were performed at 22 °C.

During the compression tests, the parts were progressively deformed until densification. The observed failure mechanism was highlighted by a shear band approximately at 45° (see Figure 1d).

3. RESULTS AND DISCUSSIONS

All parts were subjected to dimensional investigations, and non-conforming parts were replaced. Dimensional measurements were performed at three distinct locations on each sample (both extremities and the central region) using a caliper, and the mean value of these measurements was subsequently considered for analysis. Figure 2 shows the dimensional relative errors of the FFF-printed parts. It can be easily seen that the errors are very small, an aspect due to the high quality of the parts. The largest errors are found for parts C10 (0.2-0.4%), and the smallest for C30 (0-0.03%). Dimensional relative errors were calculated with Eq. (1).

$$Dimensional\ relative\ error\ [\%] = \frac{|d_m - d_n|}{d_n} \times 100 \tag{1}$$

where d_m and d_n are the measured and nominal dimensions of the parts, respectively.

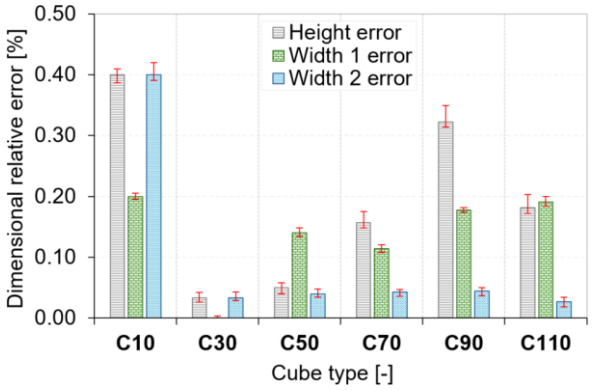

Fig. 2 – Height and width dimensional relative errors of the FFF-printed PLA parts

It was obtained that the time to print the parts increases polynomially with the increase in the size of the cube (Figure 3a), according to Eq. (2).

$$Print\ time\ [min] = 0.1810x^2 - 6.9046x + 77.5510, with\ R^2 = 0.9981 \quad (2)$$

Regardless of the size of the 3D-printed PLA parts, their masses (measured and theoretical) differ (Figure 3b). For all dimensions of the cube, the measured mass is less than the theoretical mass. A percentage difference of 6.5% was found between the two masses. Both masses increase polynomially with the increase of the side of the cube.

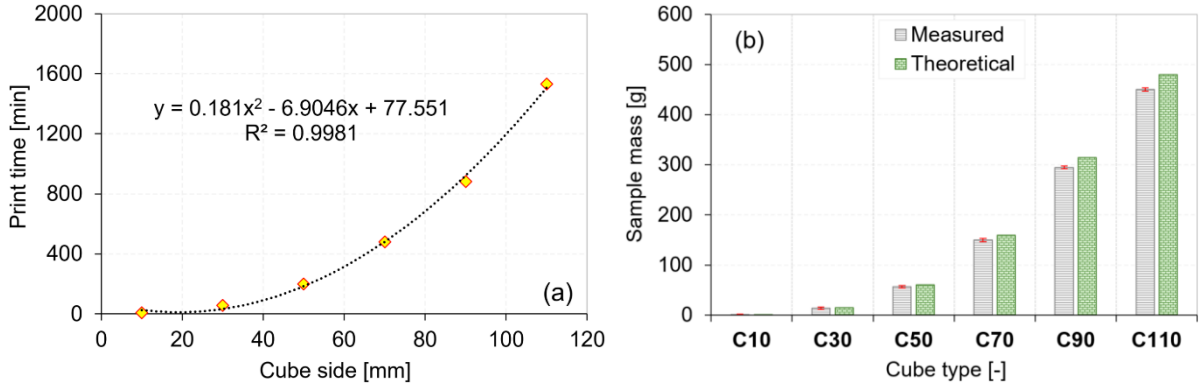

Fig. 3 – Time and mass variation of the FFF-printed PLA parts

Figure 4 presents the most representative stress-strain and energy absorption-strain curves of the FFF-printed parts. The absorbed energy was quantitatively evaluated by calculating the integral of the stress-strain response, corresponding to the area beneath the experimental curve [26]. Both sets of curves are presented up to a strain of 30%. It was noted that the compression behavior is significantly influenced by the scale effect. Moreover, the characteristics of the C10 part are clearly superior to the others. The largest cubes (C50-C110), show a more pronounced grouping of behaviors both in terms of stress and energy absorption. It was observed that the linear elastic zone does not show major differences in slope, but more in length (Figure 4a). Even so, for C50-C110 cubes this is almost similar. The major difference is recorded in the stress amplitude. Regardless of the size of the cube, the linear-elastic zone (<5% strain) does not absorb much energy, this being found in the area of plastic deformations (>7% strain), Figure 4b.

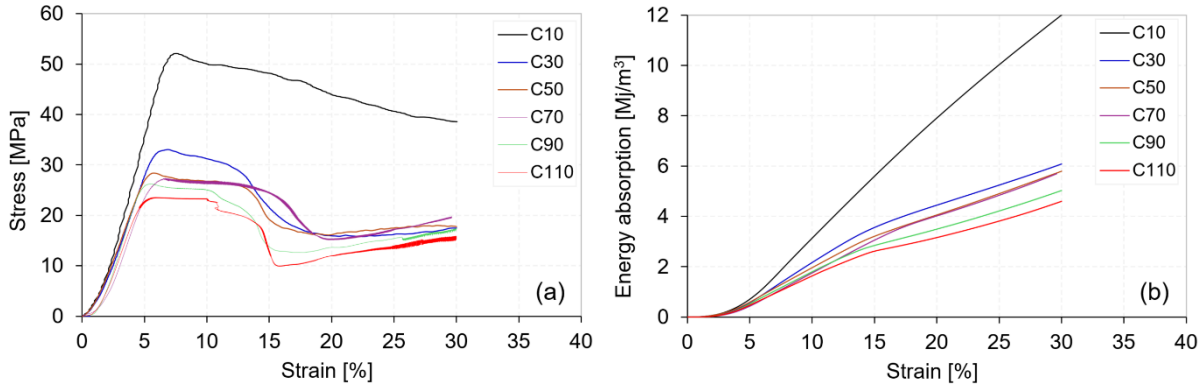

Fig. 4 – Stress-strain (a) and energy absorption-strain (b) curves of the FFF-printed PLA parts

The variation of the main compression characteristics (compressive modulus, compressive strength, minimum stress, strain at strength, energy absorption and stress amplitude) of the FFF-printed parts is presented in Figure 5.

Due to the similarities of the linear-elastic areas of the characteristic curves (see Figure 4), it was found that the compressive modulus does not present major differences (Figure 5a). The highest value, of 894.57 MPa, is given by part C10. However, a slight tendency of its decrease with the increase of the cube is observed. The lowest modulus value is given by the C50 cube (663.15 MPa).

The compressive strength decreases significantly from the smallest cube to the largest (Figure 5b). The values drop sharply from C10 to C30, followed by a smooth and linear decrease from C30 to C110. The dimensionally extreme cubes have the values of 52.10 MPa and 23.58 MPa for C10 and C110, respectively. It was found that the C50-C90 cubes have very close strength values, these being in the range of 26.2-28.4 MPa. The major difference, of 57.6%, was noted between C10 and C30 cubes, and the smallest between C50-C70 (3.6%).

A noticeable decrease (27.2%) between the dimensionally extreme cubes was also obtained in the case of strain at strength (Figure 5c). In this case, the maximum (7.53%) and minimum (5.45%) strain values were recorded by C10 and C90 cubes.

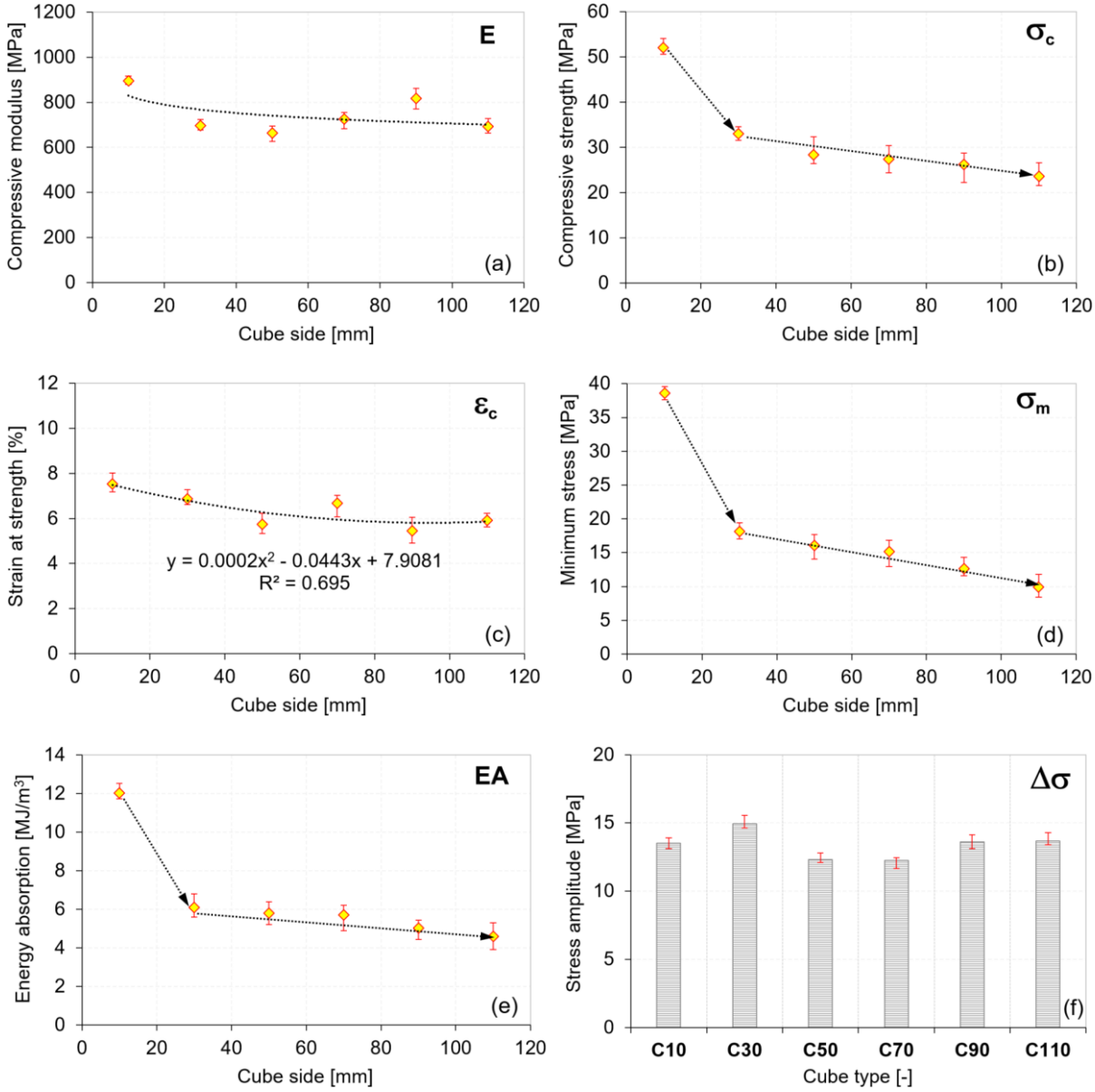

Fig. 5 – Main properties of the FFF-printed PLA parts

Minimum stress and energy absorption show similar patterns and will be discussed together (Figures 5d and 5e). Regardless of the property, the maximum values are obtained by the C10 cube (38.59 MPa for minimum stress and 12.02 MJ/m3 for energy absorption), and the minimum by the C110 (9.90 MPa for minimum stress and 4.60 MJ/m3 for energy absorption). The major drop in the decrease of the two properties is found between C10 and C30 (113.1% for minimum stress and 97.6% for energy absorption), after which the decrease is smoother and linear.

The highest stress amplitude value is identified for cube C30 (14.94 MPa), and the lowest for C70 (12.25 MPa). Stress amplitude was determined as the difference between compressive strength and minimum stress for each individual cube. Thus, between the extreme values, a percentage difference of only 10.3% is obtained.

4. CONCLUSIONS

The work presents the scale effect on the compression behavior of FFF-printed PLA parts. Following the investigations, it can be concluded:

- The 3D-printed parts presented a very high dimensional accuracy with errors below 0.4% for all three dimensions.
- The mass of the parts increases polynomially with the cube side, the measured mass being approximately 6.5% lower than the theoretical one.
- The compression characteristics are significantly influenced by the scale effect of the printed parts.
- The highest properties are obtained for the cubic part with a side of 10 mm (C10), and the lowest for the one with a side of 110 mm (C110).
- Compressive strength and strain at strength decrease polynomially with the increase of the cube side from C10 to C110, obtaining percentage differences between extremes of 120.9% for strength and 27.2% for strain.
- The compressive modulus shows fluctuations with the variation of the side of the cube, however, a decrease was noted with the increase of the part size. The extreme modulus values were found for C10 (894.57 MPa) and C50 (663.15 MPa).
- Minimum stress and energy absorption follow the same pattern, showing a percentage decreases of 289.9% for stress and 161.3% energy.
- The cubic parts were plastically deformed, highlighting a shear band as the main failure mechanism.

The scale effect should not be neglected because it is important for the extrapolation of data obtained in the laboratory on standardized parts to large engineering structures. Therefore, it is very important to find correlations in the increase/decrease of properties with the scale effect.

REFERENCES

[1] Sava R, Apostol DA, Constantinescu DM. Evaluation of the mechanical behavior of 3D printed cellular metamaterials with special geometries. Proc Rom Acad Ser A - Math Phys Tech Sci Inf Sci 2023;24(1):61-70. doi.org/10.59277/PRA-SER.A.24.1.08.

[2] Nanjundaiah RS, Rao SS, Praveenkumar K, et al. Fretting wear behavior on LPBF processed AlSi10Mg alloy for different heat treatment conditions. J Mater Res Technol 2024;30:4330-4346, doi.org/10.1016/j.jmrt.2024.06.148.

[3] Vălean C, Linul E, Rajak DK. Compressive performance of 3D-printed lightweight structures: Infill pattern optimization via Multiple-Criteria Decision Analysis method. Results Eng 2025;25:103936, doi.org/10.1016/j.rineng.2024.103936.

[4] Huang F, Wang S, Hou M, Di Z, LiuG. Morphology, mechanical properties and thermal behaviour of Poly(Methyl MethAcrylate-CO-N-Vinyl-2-Pyrrolidone)/Poly(Ethylene Glycol)/Multi-Walled Carbon Nanotubes nanocomposites. Proc Rom Acad Ser A - Math Phys Tech Sci Inf Sci 2024;25(2):139-46. doi.org/10.59277/PRA-SER.A.25.2.08

[5] Șerban DA, Coșa AV, Belgiu G, Negru R. Failure Locus of an ABS-Based Compound Manufactured through Photopolymerization. Polymers 2022; 14(18):3822. doi.org/10.3390/polym14183822.

[6] Vălean C, Orbulov IN, Kemény A, Linul E. Low-cycle compression-compression fatigue behavior of MEX-printed PLA parts. Eng Fail Anal 2024;161:108335. doi.org/10.1016/j.engfailanal.2024.108335.

[7] Stoia DI, Linul E. Tensile, flexural and fracture properties of MEX-printed PLA-based composites. Theor Appl Fract Mech 2024;132:104478. doi.org/10.1016/j.tafmec.2024.104478.

[8] Șerban D-A, Marșavina C, Coșa AV, Belgiu G, Negru R. A Study of Yielding and Plasticity of Rapid Prototyped ABS. Mathematics 2021; 9(13):1495. doi.org/10.3390/math9131495.

[9] Vălean C, Marsavina L, Linul E. Compressive behavior of additively manufactured lightweight structures: infill density optimization based on energy absorption diagrams. J Mater Res Technol 2024; 33:4952-4967, doi.org/10.1016/j.jmrt.2024.10.143.

[10] Vălean C, Linul E, Palomba G, Epasto G. Single and repeated impact behavior of material extrusion-based additive manufactured PLA parts. J Mater Res Technol 2024;30:1470-1481. doi.org/10.1016/j.jmrt.2024.03.150.

[11] Dudescu MC, Racz L, Vilău C. Strain analysis in a 3D printed car brake pedal by numerical and experimental methods. IOP Conf Ser Mater Sci Eng 2024;1319(1):012006, doi.org/10.1088/1757-899X/1319/1/012006.

[12] Vălean C, Baban M, Rajak DK, Linul E. Effect of multiple process parameters on optimizing tensile properties for material extrusion-based additive manufacturing. Constr Build Mater 2024;414:135015. doi.org/10.1016/j.conbuildmat.2024.135015.

[13] Valvez S, Silva AP, Reis PNB. Compressive behaviour of 3D-printed PETG composites. Aerospace 2022;9(3):124. doi.org/10.3390/aerospace9030124.
[11] Gadlegaonkar N, Bansod PJ, Lakshmikanthan A, et al. Osprey algorithm-based optimization of selective laser melting parameters for enhanced hardness and wear resistance in AlSi10Mg alloy. J Mater Res Technol 2025;36:3556-3571, doi.org/10.1016/j.jmrt.2024.12.201.
[12] Stoia DI, Linul E, Marsavina L. Mixed-mode I/II fracture properties of selectively laser sintered polyamide. Theor Appl Fract Mech 2022;121:103527. https://doi.org/10.1016/j.tafmec.2022.103527.
[16] Zisopol DG, Portoaca AI, Nae I, Ramadan I. A comparative analysis of the mechanical properties of annealed PLA. Eng Technol Appl Sci Res. 2022;12(4):8978-81. https://doi.org/10.48084/etasr.5123.
[17] Zisopol DG, Minescu M, Iacob DV. A Study on the influence of FDM parameters on the tensile behavior of samples made of PET-G. Eng Technol Appl Sci Res. 2024;14(2):13487-92. https://doi.org/10.48084/etasr.6949.
[18] Coșa AV, Negru R, Șerban DA. Development of Kagome-based functionally graded beams optimized for flexural loadings. Eur J Mech A Solids 2025;109:105474, doi.org/10.1016/j.euromechsol.2024.105474.
[19] Nenciu A, Apostol DA, Constantinescu DM. Experimental testing in 3-point bending of sandwich beams using additively manufactured loading bars. INCAS Bull 2025;17(1):43-52, doi.org/10.13111/2066-8201.2025.17.1.5.
[20] Oudah S, Al-Attraqchi H, Nassir N. The effect of process parameters on the compression property of acrylonitrile butadiene styrene produced by 3D printer. ETJ 2022;40(1):189-94. doi.org/10.30684/etj.v40i1.2118.
[21] Ali HB, Oleiwi JK, Othman FM. Compressive and tensile properties of ABS material as a function of 3D printing process parameters. RCMA. 2022;32(3):117-23. doi.org/10.18280/rcma.320302.
[22] Erdaş MU, Yıldız BS, Yıldız AR. Experimental analysis of the effects of different production directions on the mechanical characteristics of ABS, PLA, and PETG materials produced by FDM. Mater Test 2024;66(2):198-206. doi.org/10.1515/mt-2023-0206.
[23] Vidakis N, Petousis M, Karapidakis E, Mountakis N, David C, Sagris D. Energy consumption versus strength in MEX 3D printing of polylactic acid. Adv Ind Manuf Eng 2023;6:100119. doi.org/10.1016/j.aime.2023.100119.
[24] Vidakis N, Petousis M, Savvakis K, Maniadi A, Koudoumas E. A comprehensive investigation of the mechanical behavior and the dielectrics of pure polylactic acid (PLA) and PLA with graphene (GnP) in fused deposition modeling (FDM). Int J Plast Technol 2019;23(2):195-206. doi.org/10.1007/s12588-019-09248-1
[25] Cláudio R, Dupont J, Baptista R, Leite M, Reis L. Behaviour evaluation of 3D printed polylactic acid under compression. J Mater Res Technol 2022;21:4052-66. doi.org/10.1016/j.jmrt.2022.10.042.
[26] Linul E, Marsavina L, Kovacik J, Sadowski T. Dynamic and quasi-static compression tests of closed-cell aluminium alloy foams. Proc Rom Acad Ser A - Math Phys Tech Sci Inf Sci 2017;18(4):361-369.

Received October 10, 2024